Published in final edited form as:
*Toxicol Appl Pharmacol*. 2012 October 1; 264(1): 73–83. doi:10.1016/j.taap.2012.07.019.

# Increased expression of CYP4Z1 promotes tumor angiogenesis and growth in human breast cancer

**Wei Yu**[a,#], **Hongyan Chai**[b,#], **Ying Li**[a,#], **Haixia Zhao**[a], **Xianfei Xie**[a], **Hao Zheng**[a], **Chenlong Wang**[a], **Xue Wang**[a], **Guifang Yang**[c], **Xiaojun Cai**[d], **John R. Falck**[e], and **Jing Yang**[a,f,*]

[a]Department of Pharmacology, School of Medicine, Wuhan University, Wuhan 430071, China

[b]Center for Gene Diagnosis, Zhongnan Hospital, Wuhan University, Wuhan 430071, China

[c]Department of Pathology, Zhongnan Hospital, Wuhan University, Wuhan 430071, China

[d]Department of Ophthalmology, Zhongnan Hospital, Wuhan University, Wuhan 430071, China

[e]Department of Biochemistry, University of Texas Southwestern Medical Center, Dallas, Texas 75390, USA

[f]Research Center of Food and Drug Evaluation, Wuhan University, Wuhan 430071, China

## Abstract

Cytochrome P450 (CYP) 4Z1, a novel CYP4 family member, is over-expressed in human mammary carcinoma and associated with high-grade tumors and poor prognosis. However, the precise role of CYP4Z1 in tumor progression is unknown. Here, we demonstrate that CYP4Z1 overexpression promotes tumor angiogenesis and growth in breast cancer. Stable expression of CYP4Z1 in T47D and BT-474 human breast cancer cells significantly increased mRNA expression and production of vascular endothelial growth factor (VEGF)-A, and decreased mRNA levels and secretion of tissue inhibitor of metalloproteinase-2 (TIMP-2), without affecting cell proliferation and anchorage-independent cell growth in vitro. Notably, the conditioned medium from CYP4Z1-expressing cells enhanced proliferation, migration and tube formation of human umbilical vein endothelial cells, and promoted angiogenesis in the zebrafish embryo and chorioallantoic membrane of the chick embryo. In addition, there were lower levels of myristic acid and lauric acid, and higher contents of 20-hydroxyeicosatetraenoic acid (20-HETE) in CYP4Z1-expressing T47D cells compared with vector control. CYP4Z1 overexpression significantly increased tumor weight and microvessel density by 2.6-fold and 1.9-fold in human tumor xenograft models, respectively. Moreover, CYP4Z1 transfection increased the phosphorylation of ERK1/2 and PI3K/Akt, while PI3K or ERK inhibitors and siRNA silencing reversed CYP4Z1-mediated changes in VEGF-A and TIMP-2 expression. Conversely, HET0016, an inhibitor of the CYP4 family, potently inhibited the tumor-induced angiogenesis with associated changes in the intracellular levels of myristic acid, lauric acid and 20-HETE.



*Corresponding author: Jing Yang, MD, PhD, Professor and vice-director of Department of Pharmacology, School of Medicine, Wuhan University, Donghu Road, Wuhan 430071, China, yangjingliu@yahoo.com.cn, Tel: +86 27 68758665; Fax: +86 27 68759339; .
#These authors contributed equally to this work.



**Conflict of interest statement**
None of the authors have any conflict of interest.

Collectively, these data suggest that increased CYP4Z1 expression promotes tumor angiogenesis and growth in breast cancer partly via PI3K/Akt and ERK1/2 activation.

**Keywords**

Cytochrome P450; Angiogenesis; VEGF-A; TIMP-2; Breast cancer

## Introduction

Breast cancer is the leading cause of cancer-related deaths among women worldwide. Angiogenesis plays a critical role in the growth and metastasis of breast cancer (Schneider and Miller, 2005; Vona-Davis and Rose, 2009). Given the dismal prognosis for patients with breast cancer and the lack of significant improvement in overall survival with the current mainstays of targeted therapy (Reuben, et al., 2012), a better understanding of breast cancer growth and angiogenesis, with the goal of identification of novel targets for therapy, is imperative.

Growing evidence shows that breast cancer cells secrete high levels of vascular endothelial growth factor (VEGF) and matrix metalloproteinases (MMPs) (Reuben, et al., 2012). VEGF-A as a critical mediator of angiogenesis regulates most of the steps in the angiogenic cascade such as endothelial cell (EC) proliferation, migration and vascular branching. MMPs, a key family of proteases, are now strongly implicated in the process of angiogenesis and matrix degradation (Lee, et al., 2005; Hsieh, et al., 2011). In contrast, tissue inhibitors of metalloproteinases (TIMPs) within the tumor microenvironment inhibit tumor angiogenesis (Kessenbrock, et al., 2010). Angiogenesis-related molecules, such as VEGF, MMPs and TIMPs, have been utilized as prognostic factors and therapeutic targets in breast cancer (Cook and Figg, 2010; Waleh, et al., 2010).

The cytochrome P450 (CYP) 4 family enzymes are the most ancient members within the P450 superfamily, which often catalyze the hydroxylation of various fatty acids, such as arachidonic acid, myristic acid and lauric acid (Hsu, et al., 2007). 20-Hydroxyeicosatetraenoic acid (20-HETE), the principal ω-hydroxylation product of arachidonic acid by CYP4A and 4F, has been reported to serve as a second messenger in the mitogenic actions of a number of growth factors and an important mediator of vascular endothelial growth factor (VEGF)-induced angiogenesis (Chen, et al., 2005; Guo, et al., 2007; Dhanasekaran, et al., 2009). 12-Hydroxyeicosatrienoic acid (12-HETrE), a hydroxylation product of arachidonic acid metabolized by CYP4B1, also increased corneal limbal angiogenic activity mediated by VEGF (Seta, et al., 2007). Guo et al. reported CYP4A1 overexpression induced proliferation of glioma in vitro and in vivo, possibly mediated by 20-HETE (Guo, et al., 2008). Our previous study demonstrated that CYP4A11-derived 20-HETE promoted lung cancer angiogenesis by upregulation of VEGF and MMP-9 (Yu, et al., 2011). Conversely, CYP 4 inhibitors, like N-hydroxy-N'-(4-butyl-2 methylphenyl)formamidine (HET0016) and 17-octadecynoic acid, suppressed the formation of new blood vessels and tumor growth (Chen, et al., 2005; Guo, et al., 2005, 2006; Medhora, et al., 2007; Alexanian, et al., 2009; Yu, et al., 2011). Overall, these data suggest that CYP4 isoforms, including CYP4A, 4F and 4B, play important roles in tumor growth and angiogenesis, and their inhibitors are promising molecules for the treatment of cancer.

CYP4Z1, a novel CYP4 family member, was found to be frequently upregulated in primary mammary carcinoma and ovarian cancer (Rieger, et al., 2004; Downie, et al., 2005). Furthermore, CYP4Z1 overexpression was specifically associated with increasing tumor grade of breast cancer, as well as inferior patient outcome in ovarian cancer (Downie, et al.,

2005; Murray, et al., 2010). These data indicate that CYP4Z1 has been implicated in the pathogenesis of tumor progression. However, the precise role of CYP4Z1 in tumor progression is unclear. In this study, we studied the effects of increased CYP4Z1 expression on tumor angiogenesis and growth of human mammary carcinomas in vitro and in vivo.

## Materials and methods

### Chemicals

Antibodies against human CYP4Z1, CYP4F2 and CYP4B1 were purchased from Abcam, Inc (Cambridge, MA). Antibodies against human CYP4A11 were purchased from Santa Cruz, Inc (California, CA). WIT002 [20-hydroxyeicosa-6(Z), 15(Z)-dienoic acid] was synthesized by one of the authors John R. Falck. In addition, HET0016 and $d_6$-20-HETE were purchased from Cayman Chemicals (Ann Arbor, MI). ERK1/2 and Akt siRNA, and antibodies against PI3K, Akt, JNK, ERK, and p38 (including phosphorylated forms) were purchased from Cell Signaling Technology (Beverly, MA). Anti CD-34 antibody was purchased from DAKO Corporation (Carpenteria, CA). All other compounds were purchased from Sigma Chemical Co. (St. Louis, MO).

### Cell cultures and transfection

Human breast cancer cell lines (T47D, BT-474) were obtained from ATCC and maintained at 37 °C in a humidified incubator containing 5% $CO_2$. Human CYP4Z1 complementary DNA (cDNA) was obtained by RT-PCR of the RNA prepared from SK-BR-3 cells and subcloned into a pCI-neo expression Green Fluorescent Protein (GFP) (Promega, Madison, WI). pCI-neo-GFP vector was previously described (Wang, et al., 1996). The plasmid including the CYP4Z1 cDNA, or the plasmid alone was transfected into T47D and BT-474 cells with a Transfast Transfection Reagent kit (Promega). Stable transformants were selected with G418 (600 g/ml) for 4 weeks and isolated by a single cell manipulation technique. Proteins in established clones were studied.

### Tumor cell proliferation assay

CYP4Z1-transfected T47D (T47D-CYP4Z1) and BT-474 (BT-474-CYP4Z1) cells, vector-transfected cells (vector control) and untransfected cells at $4\times10^3$/well were plated into 96-well plates and incubated for 24, 48 and 72 h. 3-(4, 5-dimethylthiazol-2-yl)-5-(3-carboxymethoxyphenyl)-2-(4-sulfophenyl)-2H-tetrazolium (MTS) assays were done according to manufacturer's instructions (CellTiter 96 AQueous Assay reagent; Promega). For colony formation assay, cells were added to a base layer of 0.6% methylcellulose supplemented with 10% fetal bovine serum (FBS) and seeded onto 6-well plates at a density of 1-$2.5\times10^4$ cells per well in triplicate. After 7-10 d, anchorage-independent colonies were counted using a microscope.

### Gene expression analysis for several major angiogenesis-related molecules

T47D-CYP4Z1 and BT-474-CYP4Z1 cells, vector control and untransfected cells were plated into 6-well plates and incubated for 48 h, and then the cells were harvested. The mRNA levels of several major angiogenesis-related molecules, including VEGF-A, VEGF-B, MMP-2, MMP-9, TIMP-1 and TIMP-2 in the cells were measured by quantitative real-time polymerase chain reaction (qPCR) as previously described (Kawakami, et al., 2003; Pesta, et al., 2005; Meng, et al., 2007). Forward (F) and reverse (R) primers used were as follows: VEGF-A-F 5′-CCTCCGAAACCATGAACTTT-3′, VEGF-A-R 5′-TTCTTTGGTCTGCATTCACATT-3′; VEGF-B-F 5′-AGCACCAAGTCCGGATG-3′, VEGF-B-R 5′-GTCTGGCTTCACAGCACTG-3′; MMP-2-F 5′-TGGCGATGGATACCCCTTT-3′, MMP-2-R 5′-TTCTCCCAAGGTCCATAGCTCAT-3′;

MMP-9-F 5′-CCTGGGCAGATTCCAAACCT-3′, MMP-9-R 5′-GCAAGTCTTCCGAGTAGTTTTGGA T-3′; TIMP-1-F 5′-AGACCTACACTGTTGGCTGTGAG-3′, TIMP-1-R 5′-GACTGGAAGCCCTTTTCA GAG-3′; TIMP-2-F 5′-ATGCACATCACCCTCTGTGA-3′, TIMP-2-R 5′-CTCTGTGACCCAGTCCA TCC-3′, β-actin-F 5′-CCAAGGCCAACCGCGAGAAGATGA C-3′, β-actin-R 5′-AGGGTACATGGTGGTGCCGCCAGAC-3′. Total RNA was isolated from CYP4Z1-transfected cells and vector control using Trizol according to the manufacturer's protocol (Invitrogen). RNA concentration and purity were estimated from the optical density at 260 and 280 nm, respectively. Total RNA was subjected to cDNA synthesis using M-MLV Reverse Transcriptase. To determine mRNA expression levels, qPCR was performed on the ABI Prism 7500 Sequence Detector (Applied Biosystems). cDNA templates (2 L) were amplified in a final volume of 20 L containing the SYBR Green PCR Master mix and primer. Melt-curve analysis was used to confirm amplicon specificity. The length of the amplified product was confirmed using 2 % agarose gel electrophoresis. Relative quantification was performed using the $2^{-\Delta\Delta Ct}$ method. β-actin served as an appropriate reference gene in this experiment. Relative expression ratios were expressed as fold changes of mRNA abundance in the CYP4Z1-transfected T47D and BT-474 cells compared with vector control.

### Enzyme-linked immunosorbent assays for angiogenesis-related molecules

T47D-CYP4Z1 cells and BT-474-CYP4Z1 cells were plated at a concentration of $1.5\times10^5$ cells per well in 6-well plates. After incubation for 24h, the cells were washed with phosphate buffer (PBS), and then serum-starved overnight before treating with or without HET0016 or WIT002 at a non-toxic dose for 48 h. Vector control cells were used as negative control. Culture supernatants were collected, centrifuged to remove cellular debris, and then the levels of pro-and anti-angiogenic molecules including VEGF-A and TIMP-2 in culture supernatants were determined using ELISA kits according to the manufacturer's instructions (R&D systems).

To assess the contributions of the MAPK and PI3K/Akt signaling pathways to the CYP4Z1-mediated regulation of angiogenic molecules, T47D-CYP4Z1 cells were plated in 6-well plates and pre-treated with PI3K inhibitor (wortmannin), JNK inhibitor (SP600125), p38 MAPK inhibitor (SB203580) or ERK inhibitor (U0126) for 1 h or transient transfection of siRNA against ERK1/2 or Akt. After incubation for 24 h, the levels of angiogenic factors in culture supernatants were detected by ELISA kits. The experiment was repeated three times independently.

### Western blot analysis for protein expression

$1.5\times10^5$ T47D-CYP4Z1 cells per well were plated into 6-well plates and incubated for 24 h, and then serum-starved overnight in the presence or absence of HET0016 at a non-toxic dose for 24 h. T47D-vector cells were used as negative control. Proteins were extracted and the concentration was determined by Bradford method and 20 g of protein extracts were subjected to electrophoresis in 8% polyacrylamide slab gels and transferred to PVDF membrane, blocked with 5% nonfat milk, and probed with CYP4A11, CYP4F2, CYP4B1, CYP4Z1, PI3K, Akt, ERK, JNK, p38 (including phosphorylated forms) and β-actin antibodies. Blots were washed, incubated with a peroxidase-conjugated antibody, and chemiluminescence detection was performed using an enhanced chemiluminescence kit according to the manufacture's protocol (Thermo).

### Analysis of fatty acid and 20-HETE by gas chromatography mass spectrometry (GC/MS)

T47D-CYP4Z1 cells ($1\times10^6$ per plate) in 10-cm plates were incubated in the growth media for 1 day, washed with PBS, and then resupplied with serum-free medium in the presence or absence of HET0016 at a non-toxic dose. T47D-vector cells were used as negative control. After 2 days of incubation, cells from different treatment groups were harvested. Lipids were extracted from the cells as described above by the procedures similar to the Folch method (Folch, et al., 1957) and evaporated under nitrogen gas. After hydration by 0.5 mol/L HCl, free fatty acid was extracted by chloroform and esterified using 0.4 M methoxide/methanol and 14% boron trifluoride methanol. To monitor the recovery rate, the fatty acid C17:0 was added as an internal standard to the samples. All samples were separated through a capillary column (DB-WAX, 30 m×0.25mm; film thickness, 0.25 m, USA) and analyzed by an Agilent Technologies 6890N Network gas chromatograph coupled to an Agilent Technologies 5973 Network quadrupole mass selective spectrometer (Agilent, USA).

The cells as described above were harvested, pelleted, and snap-frozen in liquid $N_2$, and then homogenized in 10 l of phosphate buffer (pH 7.4). $d_6$-20-HETE that served as an internal standard was added to the homogenate sample, acidified (pH 3.5), extracted with ethyl acetate, and dried under a stream of $N_2$ gas. Pentafluorobenzyl esters and trimethylsilyl ethers were formed as previously described (Nithipatikom, et al., 2001). 20-HETE was measured by GC/MS as previously described (Rivera, et al., 2004). The ratio of peak area of m/z=391 to the peak area of m/z=397 (internal standard) was used to calculate the amount of 20-HETE in the sample.

### Effect of HET0016 on CYP4Z1 activity

T47D-CYP4Z1 cells were homogenized in a buffer containing 20 mM 4-(2-hydroxyethyl)-1-piperazineëthanesulfonic acid (HEPES), 1 mM EDTA, 100 M p-(amidinophenyl) methanesulphonyl fluoride and 250 mM sucrose. The homogenate was centrifuged at 600×g for 10 min. The supernatant was then further centrifuged at 16,000×g for 30 min. The supernatant was collected and centrifuged at 100,000×g for 30 min. The resulting pellet was were suspended in a buffer containing 50 mM Tris-HCl, 10 mM $KH_2PO_4$, 0.1 mM EDTA, 20% glycerol (pH 7.4) and stored at −80 °C for later enzymatic assays. All procedures were carried out at 4°C. The microsomal protein concentration was determined using the Folin-Lowry method. Myristic acid, lauric acid and arachidonic acid were respectively incubated with microsomal protein in the presence of 1 to 1000 nM HET0016 for 2 min at 37°C in a water bath. Metabolic reactions were initiated by the addition of 1 mM NADPH and allowed to proceed for 20 min. Reactions were quenched with 500 l of chilled 10% hydrochloric acid. Samples were extracted twice with ethyl acetate. Pooled organic extracts were dried under a $N_2$ stream and reconstituted with ethyl acetate (50 l). The same volume of N, O-bis (trimethylsily) trifluoroacetamide (BSTFA) was added to the samples, which were heated at 90°C for 45 min and analyzed by GC-MS. The $IC_{50}$ of HET0016 for CYP4Z1-dependent fatty acids hydroxylation was determined using GraphPad Prism (GraphPad Software Inc., San Diego, CA).

### Conditioned medium

Conditioned media were collected as previously described (Oh, et al., 2006). Briefly, T47D-CYP4Z1 and BT-474-CYP4Z1 cells ($1\times10^6$ per plate) in 10-cm plates were incubated in the growth media for 1 day, washed with PBS, and then resupplied with serum-free media in the presence or absence of HET0016 at a non-toxic dose. T47D and BT-474-vector cells were used as negative control. After 2 days of incubation, the conditioned media from different treatment groups of cells were harvested, and then subjected to centrifugation through an Amicon Ultra-4 filter to remove any traces of HET0016. The molecular mass cutoff of the filter was 5 kDa, and the molecular mass of HET0016 was 0.2 kDa, thus the flow-through

containing excess HET0016 was discarded, and the retentate was collected. Concentration of the conditioned media was measured by the bicinchoninic acid assay. The final filter retentate was concentrated 40-fold for several analyses, including proliferation, migration and tube formation of HUVECs, and angiogenesis in the zebrafish embryo and chorioallantoic membrane (CAM) of the chick embryo.

### Assays for in vitro proliferation, migration and tube formation of endothelial cell

Human umbilical vein endothelial cells (HUVECs; ATCC) were maintained in EGM-2 media (Clonetics, Walkersville, MD) supplemented with vascular endothelial cell growth supplement, 2% FBS, penicillin and streptomycin at 37 °C under humidified air with 5% $CO_2$. To test the effects of the conditioned media on proliferation of vascular endothelial cells, $4\times10^3$ HUVECs (in 100 l of endothelial basal medium) per well in 96-well culture plates were treated with 10 l of the conditioned media from T47D-CYP4Z1 or BT-474-CYP4Z1 cells in the presence or absence of HET0016. The conditioned medium from T47D-vector cells was used as negative control, and then the cells were incubated for 72 h. Cell viability was measured by MTS (CellTiter 96 AQueous Assay; Promega) and BrdU (Roche) incorporation assays according to manufacturer's instructions.

The HUVEC migration assay was performed in vitro using a transwell chamber (Costar) system with 8.0-μm pore polycarbonate filter inserts as described previously (Destouches, et al., 2008). HUVECs were loaded into each of the upper wells, and 30 l of the conditioned media from different treatment groups as described above were placed in upper wells. The medium supplemented with 1% FBS was then placed in the lower chamber and served as chemo-attractant. After the cells were incubated at 37 °C for 16 h, the cells on the lower surface were counted at 40 × magnification in 4 fields. Each sample was assayed in duplicate, and the experiment was repeated three times independently.

Tube formation assay was done as described (Reimer, et al., 2002). HUVECs were seeded on matrigel surfaces and grown in the absence or presence of the conditioned media (30 l) described above. After 18 h, images were photographed at ×40 magnification, and tube formation was scored by a blinded observer as follows: a three-branch point event was scored as one tube. Each condition was tested in six wells. The experiment was repeated thrice with similar results.

### Zebrafish angiogenesis assays

The effects of the conditioned medium were further assayed in vivo using the zebrafish angiogenesis model (Lee, et al., 2006). Zebrafish embryos were generated by natural pair-wise mating and maintained in embryo water (0.2 g/l of instant oceans salt in distilled water) at 28.5 °C. At 24 h post fertilization, the embryos were dechorionated and distributed into 96-well microplates, one embryo per well. Then the conditioned media from different treatment groups as noted above were added to the well. At least 20 embryos were used for each concentration. After 36 h, embryos were fixed in 4% paraformaldehyde for 2 h at room temperature. For staining, embryos were equilibrated in NTMT buffer (0.1 M Tris-HCl pH 9.5; 50 mM MgCl; 0.1 M NaCl; 0.1% Tween 20) at room temperature. Once the embryos equilibrated in NTMT, 4.5 l of 75 mg/ml NBT and 3.5 l of 50 mg/ml 5-bromo-4-chloro-3-indolyl phosphate were added. After staining for 10 min, all the blood vessels in the fish embryo were labeled and then photographed for analysis by Image Pro Plus 6.0.

### Chick embryo chorioallantoic membrane angiogenesis assay

The CAM of the chick embryo assay was performed as described previously (Connor, et al., 2005). Briefly, a window was opened above the air pocket in the shell in 9-day-old chick embryos and sealed with a piece of sterile tape. A sterile rubber O-ring was placed on the

CAM, and 10 l of conditioned media from different treatment groups as described above were placed in the center of the ring. After 48 h of incubation, a fat emulsion was injected into the CAM of the chick embryo to allow visualization of the blood vessels, and CAM was photographed with a stereomicroscope.

### Murine xenograft model of tumor growth and angiogenesis

Murine xenograft model was performed as described previously (Liang, et al., 2007). All animal studies were approved by the Animal Research Committee of Wuhan University and maintained in accordance with Association for Assessment and Accreditation of Laboratory Animal Care (AAALAC). Athymic BALB/c mice, 5-6 weeks of age (18~22 g), were provided by the Experimental Animal Center of Wuhan University and were housed on a 12-h light/12-h dark cycle in a pathogen-free environment and allowed *ad libitum* access to food and water. T47D xenografts were initiated by inoculation of 100 L cell suspension containing $5\times10^6$ T47D-CYP4Z1 or T47D-vector cells in matrigel into the right flank. Subcutaneous xenografts were maintained through slow-release estradiol pellets (0.75 mg 60-day release pellets, Innovative Research) implanted 14 days prior to cell inoculation. Three days later, the mice inoculated with T47D-CYP4Z1 cells were randomized to receive daily vehicle or HET0016 (2 mg/kg/day). The mice were examined for localized tumor, and the tumor size was measured once every two days with microcalipers. Tumor volume was calculated using the formula $0.52\times a\times b^2$, wherein a and b are the largest and smallest diameters. The mice were euthanized 2 weeks after the inoculation. The weight of each tumor was measured. Xenograft tumors were sectioned and stained using anti-CD34 antibodies. The areas of invasive tumor containing the highest numbers of capillaries and small venules per area (“hotspots”) were selected by light microscopy at low magnification (×100). After the area of the highest neovascularization was identified, individual microvessel counts were blindly made on a 400× field. Results were expressed as the mean value of all the fields.

### Statistical analysis

All values are expressed as mean ± S.D. and statistical analyses were performed using one-way ANOVA followed by the Student-Newman-Keul’s test. Values were compared using for multiple comparisons, where P values of 0.05 or less were considered significant.

## Results

### Stable expression of CYP4Z1 in human breast cancer cells does not affect cell growth in vitro

In a previous study, low mRNA levels of CYP4Z1 were detected in breast cancer cell lines such as T47D and MCF-7 (Savas, et al., 2005). However, dexamethasone induced CYP4Z1 mRNA levels by 14- and 15-fold in T47D and MCF-7 cells, respectively (Üzen Savas et al., 2006). Examination of the CYP4A11 gene regulation in HepG2 cells revealed an up to 8-fold induction of CYP4A11 mRNA by dexamethasone (Savas U et al., 2003). Our recent study found that beside CYP 4Z1, CYP4A11 and 4F2 proteins were induced by dexamethasone in a concentration-dependent manner in T47D and BT-474 cells (data not shown).Thus, the endogenous expression of CYP4Z1 induced by dexamethasone seems to be unsuitable to investigate the specific effects of CYP4Z1. We determined CYP4Z1 levels in T47D and BT-474 cells by Western blot, and found that CYP4Z1 proteins were not detectable in either T47D or BT-474 cells. Thus, we first attempted to construct overexpression systems of CYP4Z1 in T47D and BT-474 cells to study the precise role of CYP4Z1 in human mammary carcinoma progression. As shown in Fig. 1A, CYP4Z1 protein levels were significantly increased in T47D-CYP4Z1 and BT-474-CYP4Z1 cells compared with vector control. The qPCR results also exhibited approximately 60-80 fold greater

CYP4Z1 mRNA levels relative to CYP4A11, 4F2 and 4B1 in the two CYP4Z1 overexpressing-cells (Fig. 1B). Thus, we chose the two overexpression systems of CYP4Z1 for most subsequent experiments. We examined cell proliferation by MTS (Fig. 1C) and colony formation assays (Fig. 1D), and found there were no significantly differences in cell viability and colony-forming capacity between CYP4Z1-transfected cells and vector control cells, suggesting the introduction of CYP4Z1 into T47D and BT-474 cells do not affect cell proliferation and anchorage-independent growth of tumor cells.

### CYP4Z1 overexpression regulates VEGF-A and TIMP-2 levels

Accumulating evidence suggests that the regulatory influence of CYP4 enzymes including CYP4A, 4F and 4B on angiogenesis involves actions on the angiogenic factors including VEGF and MMP-9 (Seta, et al., 2007; Chen, et al., 2011; Yu, et al., 2011). Thus, we analyzed the mRNA levels of several major angiogenesis-related molecules in breast cancer cells transfected with CYP4Z1 using qPCR. VEGF-A mRNA levels were significantly elevated in CYP4Z1-expressing T47D and BT-474 cells relative to vector control, while TIMP-2 mRNA levels were significantly decreased in T47D- and BT-474-CYP4Z1 cells. The mRNA levels of several other pro-and anti-angiogenic factors such as VEGF-B, MMP-2, MMP-9 and TIMP-1 showed no difference in CYP4Z1 transfected cells compared with vector control (Fig. 2A). And then, VEGF-A and TIMP-2 protein levels were analyzed by ELISA. VEGF-A concentration was higher in culture supernatants from T47D- and BT-474-CYP4Z1 cells than vector control, while TIMP-2 concentration in culture supernatants from CYP4Z1-expressing cells was lower relative to vector control. Together, these data suggest that CYP4Z1 overexpression alters the levels of angiogenic factors including VEGF-A and TIMP-2 in breast cancer cells.

The P450 inhibitor, HET0016, is a potent and selective inhibitor of CYP4 isoforms exhibiting $IC_{50}$s in the low nanomolar region (Seki, et al., 2005). Because CYP4Z1 but no CYP4A11, 4F2 and 4B1 proteins were overexpressed in T47D-CYP4Z1 and BT-474-CYP4Z1 cells, we attempted to use 100 nM HET0016 to further investigate whether CYP4Z1 was involved in regulation of VEGF-A and TIMP-2. HET0016 was reported to have an inhibitory effect on the proliferation of human glioblastoma tumors (Guo, et al., 2008). Therefore, MTS assay was performed to investigate the effects of HET0016 on the viability of T47D- and BT-474-CYP4Z1 cells. We found that HET0016 also inhibited the proliferation of the two cell lines at a concentration of more than 1 M (data not shown). Thus, we chose 100 nM HET0016 for most subsequent experiments. ELISA assays revealed that HET0016 at a non-toxic dose partially reversed the changes in the expression levels of VEGF-A and TIMP-2 afforded by CYP4Z1 overexpression (Fig. 2B). In addition, WIT002, an antagonist of CYP4-derived-20-HETE, significantly inhibited CYP4Z1-induced VEGF-A expression in CYP4Z1-expressing T47D and BT-474 cells by 22.0 % and 32.1 %, respectively, without effecting TIMP-2 level. These data suggest the effects of HET0016 and WIT002 on the levels of VEGF-A and TIMP-2 may result from the inhibition of CYP4Z1.

### CYP4Z1 overexpression promotes tumor-induced proliferation, migration and tube formation of HUVECs

Increased expression of angiogenic factors in the tumor cells contributes to the development of the tumor vasculature (Bhat and Singh, 2008). Therefore, we further investigated whether CYP4Z1 had the pro-angiogenic activities. First, we tested its effects on endothelial cell proliferation by MTS and BrdU incorporation assay. The extent of endothelial cell proliferation over 72 h was significantly increased in the groups treated with the conditioned medium from T47D-CYP4Z1 or BT-474-CYP4Z1 cells compared with vector control (Fig. 3A). Second, transwell migration assays were conducted to access the migration abilities of

endothelial cells because migration of endothelial cells has been shown to have an important early role in neovascularization (Sudhakar, et al., 2005). When the conditioned medium from T47D-CYP4Z1 or BT-474-CYP4Z1 cells was added to the bottom chamber, the numbers of migrating HUVECs were significantly increased compared with vector control (Fig. 3B). Finally, we conducted a tube formation assay with HUVECs. As shown in Fig. 3C, the conditioned medium from T47D-CYP4Z1 and BT-474-CYP4Z1 cells significantly stimulated capillary tube formation of HUVECs on Matrigel-coated culture plates compared with the conditioned medium from T47D or BT-474-vector cells. In contrast, treatment of T47D-CYP4Z1 and BT-474-CYP4Z1 cells with HET0016 significantly inhibited tumor-induced HUVECs proliferation, migration and tube formation. Together, CYP4Z1 overexpression promotes tumor-induced HUVECs proliferation, migration and tube formation in vitro.

### CYP4Z1 overexpression promotes angiogenesis in the zebrafish embryo and CAM of the chick embryo

Capillary development in the zebrafish embryo and CAM of the chick embryo models are widely adopted methods for studying angiogenesis (Savas, et al., 2005). We used these models to investigate the pro-angiogenic activity of CYP4Z1 in vivo. The conditioned medium from T47D-CYP4Z1 cells clearly increased vessel length by 56 % in the zebrafish model (Fig. 4A), and also resulted in an increase by 59 % in the development of new embryonic blood vessels as compared with vector control in the CAM model (Fig. 4B). Conversely, the pro-angiogenic activity of CYP4Z1 was significantly inhibited by HET0016 treatment. These observations demonstrate that CYP4Z1 overexpression effectively promotes the formation of blood vessels in the zebrafish embryo and CAM of the chick embryo models.

### CYP4Z1 overexpression enhances angiogenesis and growth of T47D breast cancer xenografts in nude mice

A follow-up study was designed to validate our findings in tumor model xenografted in athymic mice. Mice inoculated with T47D-CYP4Z1 cells showed significantly enhanced tumor growth rate compared with that injected with T47D-vector cells (Fig. 5A, 5B). At the end of the second week, all animals were euthanized, and no metastatic tumor was observed in any organs. Tumor weight increased 2.6-fold in T47D-CYP4Z1 groups compared with T47D-vector groups (Fig. 5C). In contrast, treatment with HET0016 led to significant inhibition of tumor growth. Given the pro-angiogenic activities of CYP4Z1 in vitro and in vivo, we hypothesized that the promotion of growth was partly due to a secondary effect via enhanced tumor angiogenesis. We stained sections of solid tumors from the xenograft mouse model using an anti-CD34 antibody as a marker for blood vessels. Capillary vessel counting in and around primary tumors showed that CYP4Z1 overexpression significantly increased microvessel density (MVD) by 1.9-fold, while HET0016 attenuated the effect of CYP4Z1 on tumor angiogenesis by 57.9 % (Fig. 5D). These results suggest that increased CYPZ1 expression enhances human mammary carcinoma growth in vivo, at least in part, via upregulating angiogenesis.

### CYP4Z1 overexpression regulates the levels of fatty acids and 20-HETE in breast cancer cells

To further investigate the mechanisms by which CYP4Z1 overexpression promote tumor growth and angiogenesis in breast cancer, the contents of saturated fatty acids (C12:0, C14:0, C16:0, C18:0, C20:0) and unsaturated fatty acids (C18:2, C18:3, C20:2, C20:4, C20:5) were detected in breast cancer cells. Myristic (C12:0) acid, lauric acid (C14:0) and 11,14-eicosadienoic acid (C20:2) contents were significantly decreased in T47D-CYP4Z1 groups compared with T47D-vector groups, whereas there were no significant differences in

arachidonic acid levels between the two groups. Conversely, myristic (C12:0) acid and lauric acid (C14:0) contents in HET0016 treatment groups were significantly increased compared with T47D-CYP4Z1 groups (Fig. 6A). We also detected 20-HETE contents by GC-MS and found the 20-HETE levels were higher in 47D-CYP4Z1 cells than in T47D-vector cells. In contrast, 20-HETE contents in HET0016 treatment groups were lower than in T47D-CYP4Z1 groups (Fig. 6B). Together, it is possible that metabolism of fatty acids, including C12:0, C14:0, C20:2 and C20:4 (precursor of 20-HETE) by CYP4Z1 are involved in tumor growth and angiogenesis in breast cancer.

To further clarify whether the pro-angiogenic effects of CYP4Z1 might be mediated via metabolism of endogenous lipid mediators including saturated fatty acids (myristic acid and lauric acid) and unsaturated fatty acid (arachidonic acid), we evaluated the inhibitory potency of HET0016 toward CYP4Z1-mediated metabolism of fatty acids by microsomes from T47D-CYP4Z1 cells. Our data showed that $IC_{50}$ values for inhibition of 7-, 8-, 9-, 10-hydroxylase activities for lauric acid by HET0016 were 2175, 322, 523 and 168 nM, respectively. The $IC_{50}$ values for inhibition of 9-, 10-, 11-, 12-hydroxylase activities for myristic acid were 286, 549, 241 and 169 nM, respectively. We also measured the inhibitory effects of HET0016 on CYP4Z1-mediated metabolism of arachidonic acid and found that inhibition of 20-HETE metabolite formation by HET0016 was concentration-dependent with an $IC_{50}$ of 29.8 nM (Fig. 6C). These results suggest that CYP4Z1 metabolizes endogenous lipid mediators including saturated and unsaturated fatty acids, which may be involved in tumor angiogenesis and growth of human mammary carcinoma.

### The pro-angiogenic effects of CYP4Z1 are asssociated with the activation of PI3K/Akt and ERK1/2 pathways

MAPK/ERK and PI3K/Akt pathways are frequently activated in breast cancer and strongly relevant to growth and angiogenesis of breast cancer (Savas, et al., 2005). Therefore, we investigated whether CYP4Z1 overexpression could affect the activation of MAPK and PI3K/Akt signaling cascades in T47D breast cancer cell line. Increased CYP4Z1 expression significantly induced the activation of ERK1/2 and PI3K/Akt as shown by increasing the phosphorylated ERK1/2 and PI3K/Akt without affecting phospho-JNK1/2 and phospho-p38 (Fig. 7A). To further confirm whether the effects of CYP4Z1 mainly occurred through the induction of the ERK1/2 or PI3K/Akt signaling pathway, T47D cells were pretreated with a PI3K inhibitor (wortmannin), JNK inhibitor (SP600125), p38 MAPK inhibitor (SB203580) or ERK inhibitor (U0126) for 1 h or transiently transfected with siRNA against ERK1/2 or Akt, and then incubated for 24 h. We found that treatment of T47D cells with U0126, wortmannin and siRNA against ERK1/2 or Akt markedly abrogated CYP4Z1-mediated VEGF-A and TIMP-2 expression (Fig. 7B and C). Our data indicate that the pro-angiogenic effects of CYP4Z1 are asssociated with the activation of PI3K/Akt and ERK1/2 pathways.

## Discussion

Two novel observations have been made in the present study. First, we found that stable expression of CYP4Z1 in breast cancer cells promoted tumor angiogenesis evidenced by in vitro HUVECs model and in vivo CAM of the chick embryo and zebrafish models. The mouse xenograft tumor model further confirmed that CYP4Z1 overexpression enhanced tumor angiogenesis and in vivo growth of breast cancer. To our knowledge, this is the first study that directly demonstrated the pro-angiogenic property of CYP4Z1 contributing to tumor growth. Second, we have demonstrated for the first time that CYP4Z1 overexpression led to increased VEGF-A and decreased TIMP-2 expression, at least partly via ERK1/2 and PI3K/Akt activation. These results provide novel mechanistic views on the effects of CYP4Z1 on breast cancer progression.

As CYP4A, 4B and 4F with fatty acids hydroxylase acitivities exhibit pro-angiogenic effects, it is obvious to test whether CYP4Z1 in breast cancer cells displays such activities. Our data showed that the conditioned medium from CYP4Z1-expressing cells significantly enhanced proliferation, migration and tube formation of HUVECs. Given that the basic vascular plan of the developing zebrafish embryo shows strong similarity to that of mammals (Lawson and Weinstein, 2002), Zebrafish embryo, as a powerful new model system which represents a novel tool for investigating the neovascularization process, is exploitable for drug discovery and gene targeting in tumor angiogenesis (Tobia, et al., 2011). Here, the conditioned medium from T47D-CYP4Z1 cells increased blood vessel density in the zebrafish model compared with that from vector control. In addition, in the CAM of the chick embryo model, we demonstrated CYP4Z1 overexpression significantly increased new embryonic blood vessels. In a murine subcutaneous xenograft model, we showed that increased CYP4Z1 expression in T47D cells leads to increased tumor growth and angiogenesis. Conversely, the pro-angiogenic activities of CYP4Z1 were significantly inhibited by HET0016 treatment in the four models. These experiments demonstrated that CYP4Z1 overexpression promotes tumor-induced angiogenesis in breast cancer.

The angiogenesis is a dynamic process regulated by a number of pro-and anti-angiogenic molecules. VEGF-A, a crucial regulator of physiological and pathological angiogenesis, correlates with tumor progression and poor outcome in mammary carcinoma (Schneider and Miller, 2005). MMPs and TIMPs are involved in tissue remodeling and decisively regulate tumor progression including angiogenesis (Bourboulia and Stetler-Stevenson, 2010; Chandrashekar, et al., 2012). In this study, we found that CYP4Z1 overexpression significantly enhanced VEGF-A expression and downregulated TIMP-2 levels. In comparison, HET0016 at a non-toxic dose partially reversed the changes in the expression levels of VEGF-A and TIMP-2 afforded by CYP4Z1 overexpression. Furthermore, WIT002, an antagonist of CYP4-derived-20-HETE, significantly inhibited CYP4Z1-induced VEGF-A expression in CYP4Z1-expressing T47D and BT-474 cells by 22.0 % and 32.1 %, respectively, without effecting TIMP-2 level, suggesting that CYP4Z1-derived 20-HETE plays an important role in the regulation of VEGF-A. Because in our experiments there is not direct contact between tumor cells and endothelial cells, the pro-angiogenic effect of CYP4Z1 should be mediated by the angiogenesis-related molecules (VEGF-A and TIMP-2) released from tumor cells.

It was reported that the CYP4Z1-expressing fission yeast metabolized both lauric acid and myristic acid to four products (Zollner, et al., 2009). Similarly, we found that CYP4Z1 overexpression significantly decreased the levels of lauric and myristic acid in breast cancer cells, suggesting both of them could be metabolized by human breast cancer cells expressing CYP4Z1. It is well known that lauric acid and myristic acid are endogenous inhibitors of N-myristoyltransferase (NMT) (Selvakumar, et al., 2007). Furthermore, NMT exhibits distinct catalytic properties to myristoylate proteins such as a member of the Src family of tyrosine kinases, which is associated with tumor development and progression including angiogenesis (Summy and Gallick, 2003; Lieu and Kopetz, 2010). Therefore, we speculate that the decreased levels of lauric and myristic acid in breast cancer cells by CYP4Z1-mediated metabolism of saturated fatty acids will release NMT activities to myristoylate these signaling proteins contributing to tumor growth and angiogenesis. Further experiments will be carried out to elucidate the underlying mechanisms.

20-HETE, a metabolite of arachidonic acid by CYP4A and 4F, has been reported to serve as an important mediator in VEGF mediated angiogenesis (Chen, et al., 2011). Our previous study also demonstrated that CYPω-hydroxylase-derived 20-HETE promoted angiogenesis and metastasis associated with an increase of VEGF and MMP-9 in non-small lung cancer cells (Yu, et al., 2011). Thus, we detected the contents of arachidonic acid and 20-HETE in

breast cancer cells transfected with vector or CYP4Z1, and found that 20-HETE levels were higher in CYP4Z1 transfected groups than in the vector groups, whereas there were no significant differences in arachidonic acid levels between the two groups. An explanation for this discrepancy is higher sensitivity and relative efficiency in detecting a product (20-HETE) than a substrate (arachidonic acid). These data suggest that 20-HETE, a possible metabolite of arachidonic acid by CYP4Z1, at least partially contributes to angiogenesis in breast cancer.

Accumulating evidence indicates that HET0016 not only inhibited proliferation and tube formation of HUVECs (Chen, et al., 2005), but also decreased tumor growth through inhibiting the proliferation of human glioblastoma tumors (Guo, et al., 2008). Our previous study showed HET0016 inhibited human non-small cell lung cancer angiogenesis and metastasis through inhibition of CYP4A11 and CYP4F2-derived 20-HETE. In the present study, HET0016 potently inhibited the tumor angiogenesis and in vivo growth of breast cancer through reversing CYP4Z1-induced changes in angiogenic regulator (VEGF-A and TIMP-2) and endogenous lipid mediators (lauric acid, myristic acid and 20-HETE). Because CYP4Z1 but no CYP4A11, 4F2 and 4B1 protein were significantly increased in T47D-CYP4Z1 and BT-474-CYP4Z1 cells compared with vector control, the effects of HET0016 on the cells may result from the inhibition of CYP4Z1. These data suggest the potential use of HET0016 and its analogues in the treatment of human cancer by antiangiogenic mechanisms.

A number of investigators have now studied the aberrant expression of activated MAPK and PI3K/Akt in human breast cancer tissues, and found that activation of these pathways has been linked to proliferation, invasion, angiogenesis and metastasis of breast cancer (Schneider and Miller, 2005; Syed, et al., 2008; Ghayad and Cohen, 2010; McAuliffe, et al., 2010). It was reported that the role of 20-HETE in angiogenesis are mediated through MAPK and PI3K/Akt pathways (Chen, et al., 2011). Furthermore, the decreased levels of myristic acid and lauric acid will release of NMT activities which exhibits distinct catalytic properties to myristoylate proteins such as a member of the Src family of tyrosine kinases, which is associated with activation of MAPK and PI3K/Akt (Lei and Ingbar, 2011). In this study, we detected these signaling proteins by Western blot and found that CYP4Z1 overexpression significantly increased the phosphorylation of ERK1/2 and PI3K/Akt. Conversely, the changes in expression levels of VEGF-A and TIMP-2 afforded by CYP4Z1 were significantly reversed by inhibitors (U0126 and wortmannin) and siRNA silencing of ERK1/2 and PI3K/Akt in breast cancer cells. These data suggest that the activation of PI3K and ERK1/2 pathways is associated with CYP4Z1-induced angiogenesis.

In summary, our findings suggest that CYP4Z1 promotes tumor angiogenesis in human breast cancer through regulating of VEGF-A and TIMP-2 expression at least partly via PI3K and ERK1/2 activation. Specifically, it is the metabolism of endogenous lipid mediators, including saturated fatty acids (myristic acid and lauric acid) and unsaturated fatty acids (arachidonic acid) by CYP4Z1, which results in tumor angiogenesis and growth of breast cancer. These results provide strong evidence in support of the pro-angiogenic activities of CYP4Z1 in breast cancer, and targeting CYP4Z1 enzyme or CYP4Z1-derived endogenous lipid autacoids may represent a novel approach to prevent breast cancer progression.

## Acknowledgments

This work was supported by the National Natural Science Foundation of China [Grants 30973552 and 81173089] (to Jing Yang), the National Mega Project on Major Drug Development of China [Grants 2009ZX09301-014-1] (to Jing Yang) and the National Institutes of Health [Grants GM31278] (to John R. Falck).

## References


Alexanian A, Rufanova VA, Miller B, Flasch A, Roman RJ, Sorokin A. Down-regulation of 20-HETE synthesis and signaling inhibits renal adenocarcinoma cell proliferation and tumor growth. Anticancer Res. 2009; 29:3819–3824. [PubMed: 19846914]

Bhat TA, Singh RP. Tumor angiogenesis-a potential target in cancer chemoprevention. Food Chem Toxicol. 2008; 46:1334–1345. [PubMed: 17919802]

Bourboulia D, Stetler-Stevenson WG. Matrix metalloproteinases (MMPs) and tissue inhibitors of metalloproteinases (TIMPs): Positive and negative regulators in tumor cell adhesion. Semin Cancer Biol. 2010; 20:161–168. [PubMed: 20470890]

Chandrashekar N, Selvamani A, Subramanian R, Pandi A, Thiruvengadam D. Baicalein inhibits pulmonary carcinogenesis-associated inflammation and interferes with COX-2, MMP-2 and MMP-9 expressions in-vivo. Toxicol Appl Pharmacol. 2012; 261:10–21. [PubMed: 22369883]

Chen L, Ackerman R, Guo AM. 20-HETE in neovascularization. Prostaglandins Other Lipid Mediat. 2011 Epub ahead of print.

Chen P, Guo M, Wygle D, Edwards PA, Falck JR, Roman RJ, Scicli AG. Inhibitors of cytochrome P450 4A suppress angiogenic responses. Am J Pathol. 2005; 166:615–624. [PubMed: 15681843]

Connor KM, Subbaram S, Regan KJ, Nelson KK, Mazurkiewicz JE, Bartholomew PJ, Aplin AE, Tai YT, Aguirre-Ghiso J, Flores SC, Melendez JA. Mitochondrial $H_2O_2$ regulates the angiogenic phenotype via PTEN oxidation. J Biol Chem. 2005; 280:16916–16924. [PubMed: 15701646]

Cook KM, Figg WD. Angiogenesis inhibitors: current strategies and future prospects. CA Cancer J Clin. 2010; 60:222–243. [PubMed: 20554717]

Destouches D, El KD, Hamma-Kourbali Y, Krust B, Albanese P, Katsoris P, Guichard G, Briand JP, Courty J, Hovanessian AG. Suppression of tumor growth and angiogenesis by a specific antagonist of the cell-surface expressed nucleolin. PLoS ONE. 2008; 3:e2518. [PubMed: 18560571]

Dhanasekaran A, Bodiga S, Gruenloh S, Gao Y, Dunn L, Falck JR, Buonaccorsi JN, Medhora M, Jacobs ER. 20-HETE increases survival and decreases apoptosis in pulmonary arteries and pulmonary artery endothelial cells. Am J Physiol Heart Circ Physiol. 2009; 296:H777–786. [PubMed: 19136601]

Downie D, McFadyen MC, Rooney PH, Cruickshank ME, Parkin DE, Miller ID, Telfer C, Melvin WT, Murray GI. Profiling cytochrome P450 expression in ovarian cancer: identification of prognostic markers. Clin Cancer Res. 2005; 11:7369–7375. [PubMed: 16243809]

Folch J, Lees M, Sloane SGH. A simple method for the isolation and purification of total lipides from animal tissues. J Biol Chem. 1957; 226:497–509. [PubMed: 13428781]

Gebremedhin D, Lange AR, Lowry TF, Taheri MR, Birks EK, Hudetz AG, Narayanan J, Falck JR, Okamoto H, Roman RJ, Nithipatikom K, Campbell WB, Harder DR. Production of 20-HETE and its role in autoregulation of cerebral blood flow. Circ Res. 2000; 87:60–65. [PubMed: 10884373]

Ghayad SE, Cohen PA. Inhibitors of the PI3K/Akt/mTOR pathway: new hope for breast cancer patients. Recent Pat Anticancer Drug Discov. 2010; 5:29–57. [PubMed: 19751211]

Guo AM, Arbab AS, Falck JR, Chen P, Edwards PA, Roman RJ, Scicli AG. Activation of vascular endothelial growth factor through reactive oxygen species mediates 20-hydroxyeicosatetraenoic acid-induced endothelial cell proliferation. J Pharmacol Exp Ther. 2007; 321:18–27. [PubMed: 17210799]

Guo AM, Sheng J, Scicli GM, Arbab AS, Lehman NL, Edwards PA, Falck JR, Roman RJ, Scicli AG. Expression of CYP4A1 in U251 human glioma cell induces hyperproliferative phenotype in vitro and rapidly growing tumors in vivo. J Pharmacol Exp Ther. 2008; 327:10–19. [PubMed: 18591218]

Guo M, Roman RJ, Falck JR, Edwards PA, Scicli AG. Human U251 glioma cell proliferation is suppressed by HET0016 [N-hydroxy-N'-(4-butyl-2-methylphenyl)formamidine], a selective inhibitor of CYP4A. J Pharmacol Exp Ther. 2005; 315:526–533. [PubMed: 16081682]

Guo M, Roman RJ, Fenstermacher JD, Brown SL, Falck JR, Arbab AS, Edwards PA, Scicli AG. 9L gliosarcoma cell proliferation and tumor growth in rats are suppressed by N-hydroxy-N'-(4-butyl-2-methylphenol) formamidine (HET0016), a selective inhibitor of CYP4A. J Pharmacol Exp Ther. 2006; 317:97–108. [PubMed: 16352703]

Hsieh MC, Hu WP, Yu HS, Wu WC, Chang LS, Kao YH, Wang JJ. A DC-81-indole conjugate agent suppresses melanoma A375 cell migration partially via interrupting VEGF production and stromal cell-derived factor-1alpha-mediated signaling. Toxicol Appl Pharmacol. 2011; 255:150–159. [PubMed: 21708181]

Hsu MH, Savas U, Griffin KJ, Johnson EF. Human cytochrome P450 family 4 enzymes: function, genetic variation and regulation. Drug Metab Rev. 2007; 39:515–538. [PubMed: 17786636]

Kawakami M, Furuhata T, Kimura Y, Yamaguchi K, Hata F, Sasaki K, Hirata K. Expression analysis of vascular endothelial growth factors and their relationships to lymph node metastasis in human colorectal cancer. J Exp Clin Cancer Res. 2003; 22:229–237. [PubMed: 12866573]

Kessenbrock K, Plaks V, Werb Z. Matrix metalloproteinases: regulators of the tumor microenvironment. Cell. 2010; 141:52–67. [PubMed: 20371345]

Lawson ND, Weinstein BM. Arteries and veins: making a difference with zebrafish. Nat Rev Genet. 2002; 3:674–682. [PubMed: 12209142]

Lee S, Jilani SM, Nikolova GV, Carpizo D, Iruela-Arispe ML. Processing of VEGF-A by matrix metalloproteinases regulates bioavailability and vascular patterning in tumors. J Cell Biol. 2005; 169:681–691. [PubMed: 15911882]

Lee SK, Kim JM, Lee MY, Son KH, Yeom YI, Kim CH, Shin Y, Koh JS, Han DC, Kwon BM. Confirmation of a linkage between H-Ras and MMP-13 expression as well as MMP-9 by chemical genomic approach. Int J Cancer. 2006; 118:2172–2181. [PubMed: 16331612]

Lei J, Ingbar DH. Src kinase integrates PI3K/Akt and MAPK/ERK1/2 pathways in T3-induced Na-K-ATPase activity in adult rat alveolar cells. Am J Physiol Lung Cell Mol Physiol. 2011; 301:L765–771. [PubMed: 21840963]

Liang Y, Besch-Williford C, Brekken RA, Hyder SM. Progestin-dependent progression of human breast tumor xenografts: a novel model for evaluating antitumor therapeutics. Cancer Res. 2007; 67:9929–9936. [PubMed: 17942925]

Lieu C, Kopetz S. The SRC family of protein tyrosine kinases: a new and promising target for colorectal cancer therapy. Clin Colorectal Cancer. 2010; 9:89–94. [PubMed: 20378502]

McAuliffe PF, Meric-Bernstam F, Mills GB, Gonzalez-Angulo AM. Deciphering the role of PI3K/Akt/mTOR pathway in breast cancer biology and pathogenesis. Clin Breast Cancer. 2010; 10(Suppl 3):S59–65. [PubMed: 21115423]

Medhora M, Dhanasekaran A, Gruenloh SK, Dunn LK, Gabrilovich M, Falck JR, Harder DR, Jacobs ER, Pratt PF. Emerging mechanisms for growth and protection of the vasculature by cytochrome P450-derived products of arachidonic acid and other eicosanoids. Prostaglandins Other Lipid Mediat. 2007; 82:19–29. [PubMed: 17164129]

Meng F, Henson R, Wehbe-Janek H, Ghoshal K, Jacob ST, Patel T. MicroRNA-21 regulates expression of the PTEN tumor suppressor gene in human hepatocellular cancer. Gastroenterology. 2007; 133:647–658. [PubMed: 17681183]

Murray GI, Patimalla S, Stewart KN, Miller ID, Heys SD. Profiling the expression of cytochrome P450 in breast cancer. Histopathology. 2010; 57:202–211. [PubMed: 20716162]

Oh SH, Kim WY, Kim JH, Younes MN, El-Naggar AK, Myers JN, Kies M, Cohen P, Khuri F, Hong WK, Lee HY. Identification of insulin-like growth factor binding protein-3 as a farnesyl transferase inhibitor SCH66336-induced negative regulator of angiogenesis in head and neck squamous cell carcinoma. Clin Cancer Res. 2006; 12:653–661. [PubMed: 16428512]

Panigrahy D, Kaipainen A, Greene ER, Huang S. Cytochrome P450-derived eicosanoids: the neglected pathway in cancer. Cancer Metastasis Rev. 2010; 29:723–735. [PubMed: 20941528]

Pesta M, Holubec L Jr, Topolcan O, Cerna M, Rupert K, Holubec LS, Treska V, Kormunda S, Elgrova L, Finek J, Cerny R. Quantitative estimation of matrix metalloproteinases 2 and 7 (MMP-2, MMP-7) and tissue inhibitors of matrix metalloproteinases 1 and 2 (TIMP-1, TIMP-2) in colorectal carcinoma tissue samples. Anticancer Res. 2005; 25:3387–3391. [PubMed: 16101153]

Reimer CL, Agata N, Tammam JG, Bamberg M, Dickerson WM, Kamphaus GD, Rook SL, Milhollen M, Fram R, Kalluri R, Kufe D, Kharbanda S. Antineoplastic effects of chemotherapeutic agents are potentiated by NM-3, an inhibitor of angiogenesis. Cancer Res. 2002; 62:789–795. [PubMed: 11830534]

Reuben SC, Gopalan A, Petit DM, Bishayee A. Modulation of angiogenesis by dietary phytoconstituents in the prevention and intervention of breast cancer. Mol Nutr Food Res. 2012; 56:14–29. [PubMed: 22125182]

Rieger MA, Ebner R, Bell DR, Kiessling A, Rohayem J, Schmitz M, Temme A, Rieber EP, Weigle B. Identification of a novel mammary-restricted cytochrome P450, CYP4Z1, with overexpression in breast carcinoma. Cancer Res. 2004; 64:2357–2364. [PubMed: 15059886]

Rivera J, Ward N, Hodgson J, Puddey IB, Falck JR, Croft KD. Measurement of 20-hydroxyeicosatetraenoic acid in human urine by gaschromatography-mass spectrometry. Clin Chem. 2004; 50:224–226. [PubMed: 14709657]

Savas U, Hsu MH, Griffin KJ, Bell DR, Johnson EF. Conditional regulation of the human CYP4X1 and CYP4Z1 genes. Arch Biochem Biophys. 2005; 436:377–385. [PubMed: 15797250]

Schneider BP, Miller KD. Angiogenesis of breast cancer. J Clin Oncol. 2005; 23:1782–1790. [PubMed: 15755986]

Seki T, Wang MH, Miyata N, Laniado-Schwartzman M. Cytochrome P450 4A isoform inhibitory profile of N-hydroxy-N'-(4-butyl-2-methylphenyl)-formamidine (HET0016), a selective inhibitor of 20-HETE synthesis. Biol Pharm Bull. 2005; 28:1651–1654. [PubMed: 16141533]

Selvakumar P, Lakshmikuttyamma A, Shrivastav A, Das SB, Dimmock JR, Sharma RK. Potential role of N-myristoyltransferase in cancer. Prog Lipid Res. 2007; 46:1–36. [PubMed: 16846646]

Seta F, Patil K, Bellner L, Mezentsev A, Kemp R, Dunn MW, Schwartzman ML. Inhibition of VEGF expression and corneal neovascularization by siRNA targeting cytochrome P450 4B1. Prostaglandins Other Lipid Mediat. 2007; 84:116–127. [PubMed: 17991614]

Sudhakar A, Nyberg P, Keshamouni VG, Mannam AP, Li J, Sugimoto H, Cosgrove D, Kalluri R. Human alpha1 type IV collagen NC1 domain exhibits distinct antiangiogenic activity mediated by alpha1beta1 integrin. J Clin Invest. 2005; 115:2801–2810. [PubMed: 16151532]

Summy JM, Gallick GE. Src family kinases in tumor progression and metastasis. Cancer Metastasis Rev. 2003; 22:337–358. [PubMed: 12884910]

Syed DN, Afaq F, Sarfaraz S, Khan N, Kedlaya R, Setaluri V, Mukhtar H. Delphinidin inhibits cell proliferation and invasion via modulation of Met receptor phosphorylation. Toxicol Appl Pharmacol. 2008; 231:52–60. [PubMed: 18499206]

Tobia C, De Sena G, Presta M. Zebrafish embryo, a tool to study tumor angiogenesis. Int J Dev Biol. 2011; 55:505–509. [PubMed: 21858773]

Vona-Davis L, Rose DP. Angiogenesis, adipokines and breast cancer. Cytokine Growth Factor Rev. 2009; 20:193–201. [PubMed: 19520599]

Waleh NS, Murphy BJ, Zaveri NT. Increase in tissue inhibitor of metalloproteinase-2 (TIMP-2) levels and inhibition of MMP-2 activity in a metastatic breast cancer cell line by an anti-invasive small molecule SR13179. Cancer Lett. 2010; 289:111–118. [PubMed: 19751965]

Wang DS, Miller R, Shaw R, Shaw G. The pleckstrin homology domain of human beta I sigma II spectrin is targeted to the plasma membrane in vivo. Biochem Biophys Res Commun. 1996; 225:420–426. [PubMed: 8753778]

Yu W, Chen L, Yang YQ, Falck JR, Guo AM, Li Y, Yang J. Cytochrome P450 omega-hydroxylase promotes angiogenesis and metastasis by upregulation of VEGF and MMP-9 in non-small cell lung cancer. Cancer Chemother Pharmacol. 2011; 68:619–629. [PubMed: 21120482]

Zollner A, Dragan CA, Pistorius D, Muller R, Bode HB, Peters FT, Maurer HH, Bureik M. Human CYP4Z1 catalyzes the in-chain hydroxylation of lauric acid and myristic acid. Biol Chem. 2009; 390:313–317. [PubMed: 19090726]

## Highlights

- CYP4Z1 overexpression promotes human breast cancer growth and angiogenesis.
- The pro-angiogenic effects of CYP4Z1 have been studied *in vitro* and *in vivo*.
- CYP4Z1 regulates expression and production of VEGF-A and TIMP-2.
- CYP4Z1-induced angiogenesis is asssociated with PI3K and ERK1/2 activation.
- CYP4Z1 may be an attractive target for anti-cancer therapy.

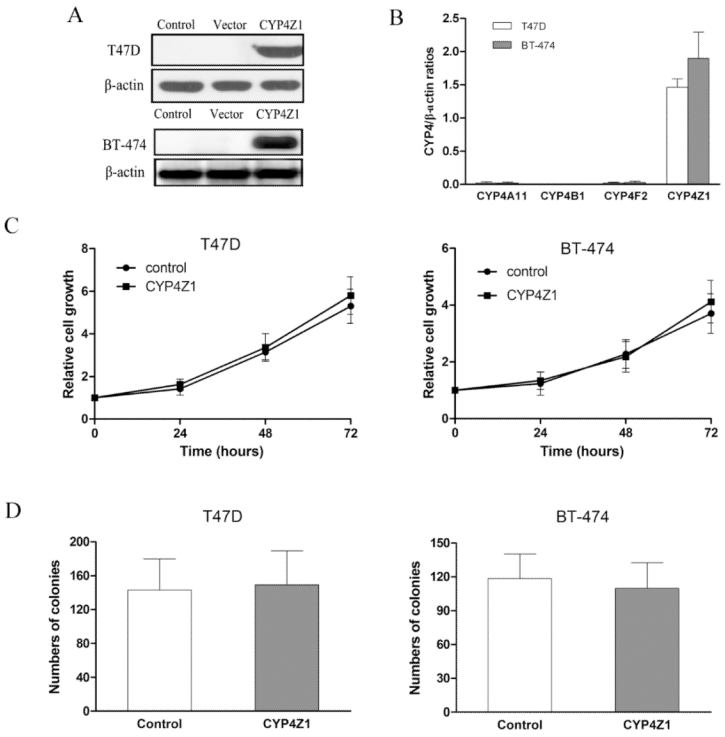


**Fig. 1.**

Stable expression of CYP4Z1 in human breast cancer cells does not affect cell proliferation and colony formation in vitro. (A) CYP4Z1 protein expression in T47D and BT-474 cells transfected or untransfected with CYP4Z1 was determined by Western blot. (B)The mRNA levels of CYP4A11, 4F2, 4B1 and 4Z1 in T47D and BT-474 cells transfected with CYP4Z1 were determined by quantitative real-time polymerase chain reaction (qPCR). (C) CYP4Z1-transfected T47D (T47D-CYP4Z1) and BT-474 (BT-474-CYP4Z1) cells and vector-transfected cells (vector control) at $4\times10^3$/well were plated into 96-well plates and incubated for 24, 48 and 72 h. Cell proliferation was determined by MTS. (D) CYP4Z1 or vector-transfected cells were added to a base layer of 0.6% methylcellulose supplemented with 10% fetal bovine serum (FBS) and were seeded onto 6-well plates at a density of $1\text{-}2.5\times10^4$ cells per well in triplicate. After 7-10 d, anchorage-independent colonies were counted using a microscope. Results are shown as mean ± S.D. from 3 independent experiments (n=3).

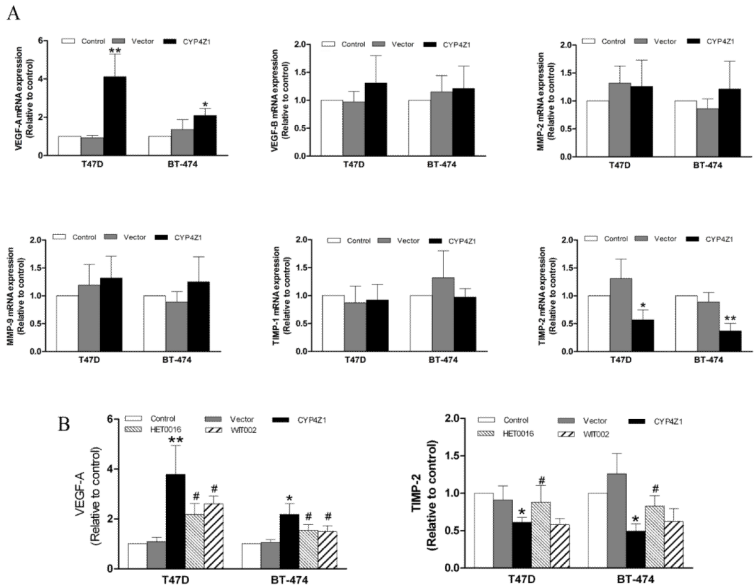


**Fig. 2.**

CYP4Z1 overexpression regulates VEGF-A and TIMP-2 levels in breast cancer cells. (A) mRNA expression of several major pro-and anti-angiogenic factors from T47D and BT-474 cells transfected or untransfected with CYP4Z1 were examined using quantitative real-time polymerase chain reaction (qPCR). Each data point is expressed as mean ± S.D. from 3 independent experiments (n=3). (B) T47D-CYP4Z1 cells and BT-474-CYP4Z1 cells were plated at a concentration of $1.5\times10^5$ cells per well in 6-well plates. After incubation for 24 h, the cells were washed with phosphate buffer, and then serum-starved overnight before treating with or without HET0016 (100 nM) or WIT002 (1 M) for 48 h. Vector control cells were used as negative control. The levels of VEGF-A and TIMP-2 in culture supernatants were determined using ELISA kits. Results are shown as mean ± S.D. from 3 independent experiments (n=3). $^*P < 0.05$, $^{**}P < 0.01$ vs. control group; $^{\#}P < 0.05$ vs. CYP4Z1 transfeciton group.

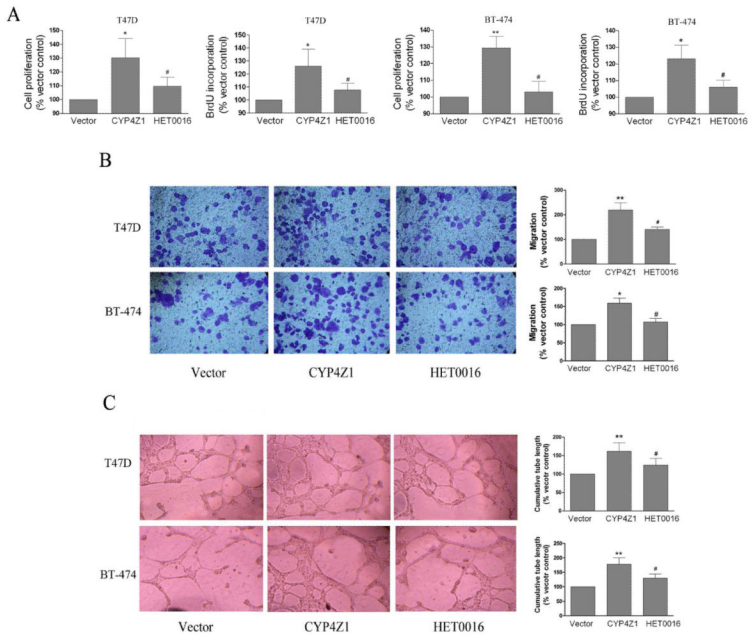


**Fig. 3.**

The conditioned medium from CYP4Z1-expressing T47D and BT-474 cells enhanced proliferation, migration and tube formation of human umbilical vein endothelial cells (HUVECs). (A) Cell proliferation. HUVECs were plated at $3\times10^3$ per well in 96-well culture plates, and then treated with the conditioned medium as in the presently described method. Cell proliferation was measured using the MTS and BrdU incorporation assays. (B) Migration assays. HUVEC migration assays were performed using culture supernatants that were derived from T47D or BT-474 cells transfected or untransfected with CYP4Z1, and cell migration was measured in a 16-h Transwell assay in a blinded manner. (C) Tube formation assays. Cells were seeded on matrigel-coated wells in the presence of different conditioned media, as indicated, and incubated for 18 h to form a capillary network. The total number of branched tubes was then counted. Results are shown as mean ± S.D. from 3 independent experiments (n=3). $^{*}P < 0.05$, $^{**}P < 0.01$ vs. vector control group; $^{\#}P < 0.05$ vs. T47D-CYP4Z1 group.

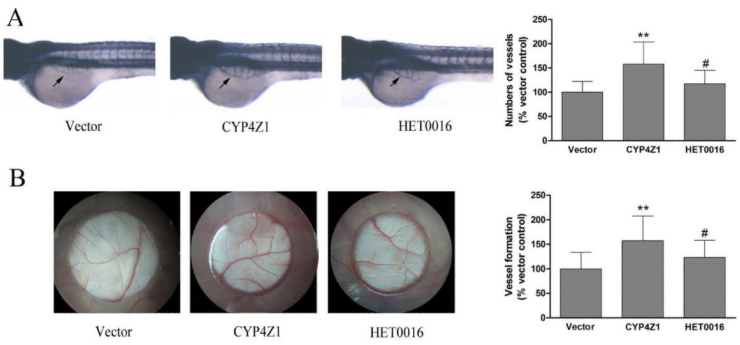


**Fig. 4.**

CYP4Z1 overexpression promotes tumor-induced angiogenesis in the zebrafish embryo and chorioallantoic membrane (CAM) of the chick embryo. (A) The embryos were dechorionated and distributed into 96-well microplates. Then the conditioned media were added to the well. At 36 h post fertilization, embryos were fixed in 4% paraformaldehyde for 2 h at room temperature and stained, and then photographed for analysis by Image Pro Plus 6.0. (B) In the CAM assay, angiogenesis stimulated by conditioned media was photograped or quantitatively evaluated. Independent experiments were repeated three times. $^{*}P < 0.05$, $^{**}P < 0.01$ vs. vector control group; $^{\#}P < 0.05$ vs. CYP4Z1 group; Results are shown as mean ± S.D. from 3 independent experiments (n=20).

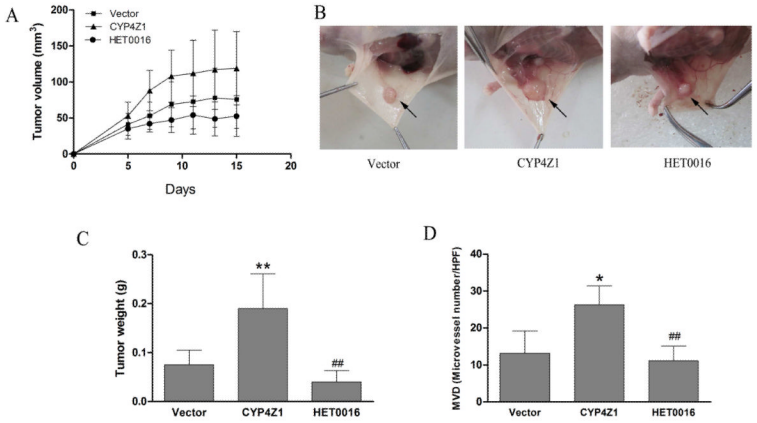


**Fig. 5.**

CYP4Z1 overexpression enhances angiogenesis and growth of T47D breast cancer xenografts in nude mice. Nude mice injected with T47D cells transfected with CYP4Z1 or vector. After 2 days, the mice were treated with or without HET0016 (2 mg/kg). (A) Primary xenograft tumor volume growth curves. (B) Selected images of xenograft tumors in different groups at the end of the experiment as shown in (A). (C) Average primary tumor weight for each group after growth for 2 weeks. (D) Average microvessel density (MVD) in primary tumors and around tumors was counted in a blinded manner (Capillary vessel number per HPF). Results are shown as mean ± S.D. (n=6). $^{**}P < 0.01$ vs. vector control; $^{\#\#}P < 0.01$ vs. T47D-CYP4Z1 groups.

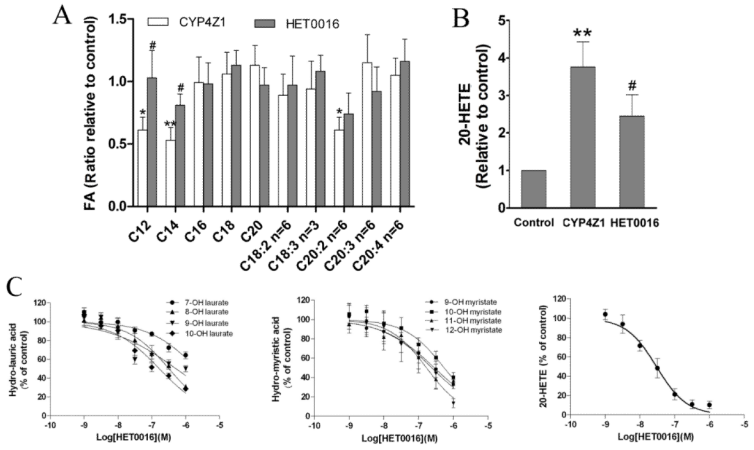


**Fig. 6.**

CYP4Z1 overexpression regulates fatty acid contents and 20-HETE production in breast cancer cells. T47D-CYP4Z1 cells and vector control cells ($1\times10^6$ per plate) in 10-cm plates were incubated in the growth media for 24 h, washed with phosphate buffer, and then resupplied with serum-free medium in the presence or absence of HET0016 (100 nM). After 2 days of incubation, the cells were subjected to GC/MS analysis for fatty acid contents (A) and 20-HETE production (B). Microsomes were isolated from T47D cells transfected with CYP4Z1, and effect of HET0016 (1-1000 nM) on CYP4Z1-catalyzed hydroxylation of lauric acid, myristic acid and arachidonic acid were assayed (C). Results are shown as mean ± S.D. from 3 independent experiments (n=3). $^{*}P<0.05$, $^{**}P<0.01$ vs. vector control; $^{\#}P<0.05$ vs. T47D-CYP4Z1 groups.

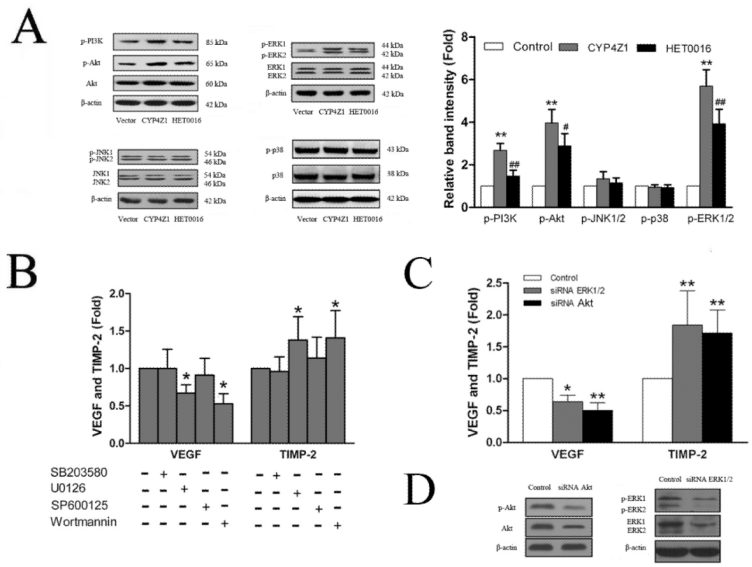


**Fig. 7.**

The pro-angiogenic effects of CYP4Z1 are associated with the activation of PI3K/Akt and ERK1/2. . (A) T47D-CYP4Z1 and T47D-vector cells were plated into 6-well plates and incubated in serum-free media in the absence or present of HET0016 for 24 h and then the cell lysates were subjected to sodium dodecyl sulfate-polyacrylamide gel electrophoresis followed by Western blot. Quantification of phospho-MAPKs and phosphor-PI3K/Akt proteins was performed by densitometric analysis of the Western blot bands shown left. (B) The effects of specific inhibitors of MAPK and PI3K/Akt on CYP4Z1-induced the expression of VEGF-A and TIMP-2. CYP4Z1-transfected T47D (T47D-CYP4Z1) cells were plated in 6-well plates and pre-treated with PI3K inhibitor (wortmannin), JNK inhibitor (SP600125), p38 MAPK inhibitor (SB203580) and ERK inhibitor (U0126) for 1 h, and then incubated for 24 h. Afterwards, the culture medium was subjected to ELISA to analyze the production of VEGF-A and TIMP-2. (C) T47D-CYP4Z1 cells were transfected with siRNA against ERK1/2, Akt or nonspecific control siRNA duplexes, and then grown for 48 h before harvest. The effects of siRNA against ERK1/2 or Akt on CYP4Z1-induced the expression of VEGF-A and TIMP-2 were determined by Western blot. (D) The effects of siRNA against ERK1/2 or Akt on the protein levels of ERK1/2 and Akt (including phosphorylated forms) were assayed by Western blot. Results are shown as mean ± S.D. from 3 independent experiments (n=3). $^{*}P < 0.05$, $^{**}P < 0.01$ vs. vector control group; $^{\#}P < 0.05$, $^{\#\#}P < 0.01$ vs. T47D-CYP4Z1 group.